

Field-induced metal-insulator transition and switching phenomenon in correlated insulators

Naoyuki Sugimoto*

Department of Applied Physics, University of Tokyo, Tokyo 7-3-1, Hongo, Tokyo 113-8656, Japan

Shigeki Onoda

Condensed Matter Theory Laboratory, The Institute of Physical and Chemical Research (RIKEN), Wako 351-0198, Japan

Naoto Nagaosa

*Department of Applied Physics, University of Tokyo, Tokyo 7-3-1, Hongo, Tokyo 113-8656, Japan
and Cross-Correlated Materials Research Group (CMRG), ASI, RIKEN, 2-1 Hirosawa, Wako, Saitama 351-0198, Japan*

(Received 8 September 2008; published 6 October 2008)

We study the nonequilibrium switching phenomenon associated with the metal-insulator transition under electric field E in correlated insulators by a gauge-covariant Keldysh formalism. Due to the feedback effect of the resistive current I , this occurs as a first-order transition with a hysteresis of I - V characteristics having a lower threshold electric field ($\sim 10^4$ V cm $^{-1}$) much weaker than that for the Zener breakdown. It is also found that the localized midgap states introduced by impurities and defects act as hot spots across which the resonant tunneling occurs selectively, which leads to the conductive filamentary paths and reduces the energy cost of the switching function.

DOI: [10.1103/PhysRevB.78.155104](https://doi.org/10.1103/PhysRevB.78.155104)

PACS number(s): 71.30.+h, 72.10.Bg, 72.20.Ht

In correlated electronic systems, the Coulomb interaction and the electron-phonon coupling give rise to various long-range orderings of spin, charge, and orbital degrees of freedom of electrons, providing rich phase diagrams and intriguing phenomena such as colossal magnetoresistance.¹ The collective response can be significantly sensitive and amplified in comparison with that in semiconductors,² because many electrons cooperate in a short length scale of nanometers owing to the high electron density. These orderings often lead to an insulating behavior with an energy gap in the single-electron spectrum represented by the Mott gap.³ In sharp contrast to the band insulators, the gap itself can be controlled by the external stimuli, as observed in experiments on the metal-insulator transition driven by the electric field^{4,5} or the light irradiation.^{6,7} Furthermore, metal-insulator switching phenomena have been observed in other correlated electronic systems such as organic charge-transfer compounds,⁸ $\text{La}_{2-x}\text{Sr}_x\text{NiO}_4$,⁹ and one-dimensional Mott insulators $\text{Sr}_2\text{CuO}_3/\text{SrCuO}_2$.¹⁰ Recently, the application of the switching phenomenon to electronic devices has also been seriously considered.¹¹ One important observation here is that the threshold electric fields observed in the correlated systems are typically 10^4 V/cm,⁹ which is much less than the $\sim 10^6$ V/cm expected from the simple Zener breakdown (see below). This suggests a positive feedback effect of the collective nature of the metal-insulator transition in the switching phenomena. Also the current is often nonuniform and confined in narrow paths or filaments.^{5,12}

Theoretically, the description of the nonequilibrium states still remains a challenge even though there are several related works.¹³⁻¹⁵ In these works, the electron correlations in the metal-insulator transition were studied by using a Hubbard-type model in the strong electric field with the open boundary conditions. The effect of strong correlations were numerically treated by using the time-dependent density-matrix renormalization-group method¹³ or the dynamical mean-field theory combined with the Keldysh Green's-

function technique.¹⁵ As a result of these calculations, these works obtained the current-voltage characteristics with one threshold electric field, which were similar to that of the semiconductor. These works assumed that the dissipation occurs only at the boundary or in the leads, which is justified for the finite-length systems. For the bulk system, on the other hand, we need to consider the relaxation processes and the dissipation within the sample. Namely, the competition between the electron correlation effect and the steady current should be studied in the presence of the dissipation induced by impurities. However, calculation of the steady state with impurities under the strong electric field has been difficult. Recently, we developed such formalism to deal with the far-from-equilibrium states.¹⁶ This enables us to microscopically incorporate the effects of the impurities into the Dyson equation for the nonequilibrium Green's function with the electric field, which is written in a compact form by using the Moyal product in the gauge-covariant Wigner representation.

In this paper, we develop a theory of the resistive switching phenomenon in the spin/charge ordered correlated insulators employing the gauge-covariant Keldysh formalism combined with the mean-field approximation to the electron-electron interaction. As shown below, the feedback effect of the current defines a threshold electric field. Namely, there exist two threshold electric fields in our theory. The threshold field plays a crucial role in the mechanism of the phase transition. We have obtained theoretically the hysteric resistive switching due to the applied electric field. Our theory also accounts for the experimentally observed low threshold field and filament formation.

We study the one-dimensional interacting electrons described by

$$\hat{H} = \sum_{p\sigma} \varepsilon(p) c_{p,\sigma}^\dagger c_{p,\sigma} + g \sum_{p_1, p_2, q} c_{p_1+q, \uparrow}^\dagger c_{p_2-q, \downarrow}^\dagger c_{p_2, \downarrow} c_{p_1, \uparrow}, \quad (1)$$

where g is assumed to be a constant and repulsive and the other notations are standard. This interaction naturally leads

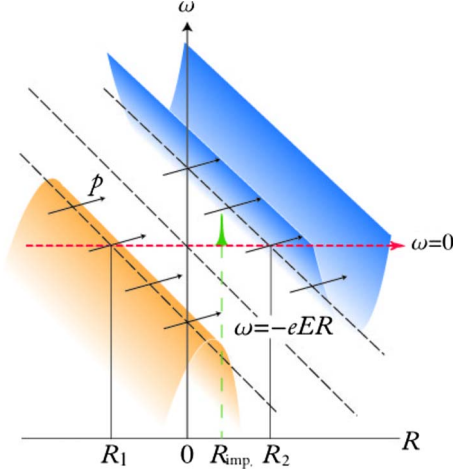


FIG. 1. (Color online) The tilted band structure under an external electric field E . At each spatial position R , the momentum p is defined as shown in the orthogonal direction. The conduction-band bottom and the valence-band top cross the energy $\omega=0$ at R_2 and R_1 , respectively. The localized impurity state represented by the peak at $R=R_{\text{imp}}$ gives rise to the resonant tunneling.

to the spin-density-wave ordering at the wave vector $2k_F$ (k_F : Fermi wave number), which is assumed to be half of the reciprocal-lattice vector G , i.e., half filling, and introduces the gap 2Δ . The sign of the gap is the opposite for the opposite spin, and we can just consider the two copies of the spinless electrons by the mean-field Hamiltonian

$$\hat{H} \cong \sum_p \vec{c}_p^\dagger \begin{pmatrix} vp & \Delta \\ \Delta & -vp \end{pmatrix} \vec{c}_p, \quad (2)$$

where $\vec{c}_p = (c_{p,R}, c_{p,L})$ is the two-component operator corresponding to the right-going and left-going electrons near $\pm k_F$ with the dispersion $\pm vp$ (v : velocity). Here, $2\Delta := g \langle c_{p,R}^\dagger c_{p,L} \rangle$ is the self-consistently determined gap [see Eq. (4)]. While this ordered state in equilibrium is well known, we are interested in the nonequilibrium phase transition driven by the electric field. Note that the ordering is commensurate, and the phason degrees of freedom is quenched in sharp contrast to the sliding charge-density-wave problem.¹⁷ The interaction is treated in the mean-field approximation, which is justified in the weak- to intermediate-coupling regime, though a more elaborate treatment is required in the strong-coupling regime.

We separate the problem into two steps, i.e., (i) describe the current flowing state under the electric field in mean-field Hamiltonian (2), and (ii) solve the self-consistent equation $2\Delta = g \langle c_{p,R}^\dagger c_{p,L} \rangle$ for the gap. The first step is basically the Zener tunneling problem studied previously.^{18–23} As schematically shown in Fig. 1, the electrons tunnel through the energy gap. The band structure is spatially tilted by the potential energy gain $-eER$, where R is the real-space position and $-e$ is the electronic charge. One can consider the locally defined band structure as a function of the momentum (which is represented along the transverse axis) at each R , and the equienergy line crosses the bottom (top) of the con-

duction (valence) band at $R=R_1$ ($R=R_2$). The wave functions of conduction and valence bands tunnel through the potential barrier between R_1 and R_2 from both sides.

There are three length scales with this problem: (i) the correlation length $\zeta = \hbar v / 2\Delta$ associated with the energy gap 2Δ , which describes the characteristic extent of the wave packet relevant to the tunneling; (ii) the tunneling length $\xi = 2\Delta / eE = R_2 - R_1$ over which an electron can gain the energy 2Δ by the electric field E ; and (iii) the mean free path ℓ . The Zener tunneling occurs quite differently depending on the relative magnitudes of these length scales. We will focus below on the case of $\ell \gg \zeta$; the mean free path is much longer than the correlation length, or the energy gap 2Δ is much larger than the energy broadening $\hbar v / \ell$ due to the impurity scatterings. Then the Zener tunneling is controlled by the ratio ξ / ζ . When $\xi \gg \zeta$, the Zener tunneling probability can be calculated in the semiclassical approximation as $\sim \exp[-\pi \xi / 2\zeta]$.²³ As we increase the electric field so that $\xi < \zeta$, the wave packet extends from R_1 to R_2 and the metallic conduction occurs, i.e., the crossover between the Zener tunneling and ohmic regions.

Although this picture is valid qualitatively, it is crucial to consider steady state with the dissipative current flowing to describe the nonequilibrium phase transition. We perform the self-consistent calculations of Green's functions and self-energies in the Keldysh space in the gauge-covariant Wigner representation, which is now composed of the mechanical energy and momentum.^{16,24} It is necessary to introduce the Green's functions and the self-energies in the Keldysh space, $\hat{G} := \begin{pmatrix} \hat{G}^R & 2\hat{G}^< \\ 0 & \hat{G}^A \end{pmatrix}$ and $\hat{\Sigma} := \begin{pmatrix} \hat{\Sigma}^R & 2\hat{\Sigma}^< \\ 0 & \hat{\Sigma}^A \end{pmatrix}$, respectively.¹⁶ Kinetic equations of the functions are given in the form of the Dyson equations:

$$(\hat{\mathcal{L}} - \hat{\Sigma}) \star \hat{G} = 1,$$

$$\hat{G} \star (\hat{\mathcal{L}} - \hat{\Sigma}) = 1,$$

with $\hat{\mathcal{L}}(\omega, p) := \omega - \hat{H}(p)$. The symbol \star denotes the Moyal product

$$(f \star g)(x) = \int \frac{dydz}{(\pi e \hbar v)^2} f(y) g(z) e^{(-2i/eE\hbar v)[(x^y - y^y)S_{\mu\nu}(x^y - z^y)]},$$

where x, y, z denote the two-dimensional energy-momentum coordinates (ω, vp) , f and g are the smooth functions of the energy momentum, and $S_{\mu\nu} := \begin{pmatrix} 0 & -1 \\ 1 & 0 \end{pmatrix}$.

Now, we turn to the calculation of $\hat{G}^{R,A}$ and $\hat{G}^<$ for the Landau-Zener model with the δ -functional random impurity potential. Let us start with the pure case of $\hat{\Sigma}^{R,A} = \mp i\eta$ with an infinitesimal number η . By using a Fourier transform, $\mathcal{F}[f](\omega, \epsilon) := \int \frac{dp}{2\pi\hbar} f(\omega, p) e^{-2ip\epsilon/\hbar eE}$, we obtain the Green's function in the pure case as

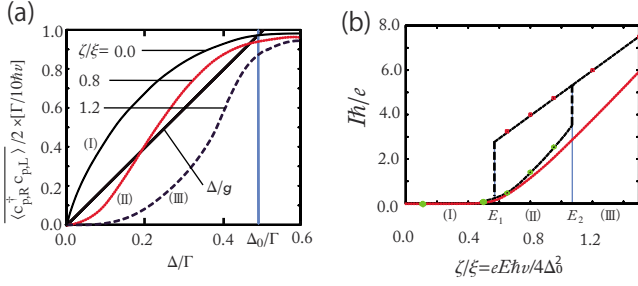


FIG. 2. (Color online) (a) The right-hand side of gap equation (4), $\langle c_{p,R}^\dagger c_{p,L} \rangle / 2$, in unit of $\Gamma / 10\hbar v$ as a function of the gap Δ for $\zeta/\xi = eE\hbar v / 4\Delta_0^2 = 0.0, 0.8, 1.2$, with Γ being the energy cutoff, i.e., the half bandwidth of the equilibrium states. Here, Δ_0 is the gap in the equilibrium for $g = 5\hbar v$. The solid straight line represents Δ/g in the same unit and the crossing of these two gives the solution(s) to mean-field equation (4). (b) The obtained current I as a function of the electric field E . The dashed line is a guide for the eyes. The I - E characteristics clearly show the hysteresis and switching behavior of the current. The red dotted curve represents the current obtained for the fixed gap Δ_0 .

$$\hat{G}_{\text{pure}}^{R,A}(\omega, p) = \sum_{s=1,2} \frac{2}{eE} \int d\epsilon dY \frac{\hat{\Phi}_s^+(Y + \epsilon) \hat{\Phi}_s^-(Y - \epsilon)}{\omega - Y \pm i\eta} e^{2ip\epsilon/eE\hbar}, \quad (3)$$

where $\hat{\Phi}_s := {}^t(\Phi_s^+, \Phi_s^-)$ are the solutions of the following Weber equations:¹⁹ $(\partial_z^2 + \frac{1}{2} \pm i \frac{\Delta^2}{2e\hbar v} - \frac{z^2}{4}) \Phi_s^\pm(\sqrt{\frac{eE\hbar v}{2}} e^{\mp i\pi/4} z) = 0$ with a normalization condition, $\sum_{s=1,2} \int d\lambda \hat{\Phi}(\lambda - \omega) \hat{\Phi}^\dagger(\lambda - \omega') = \delta[(\omega - \omega')/eE]$. We employed the self-consistent Born approximation, $\hat{\Sigma}^{R,A}(\omega) = n_i u^2 \hat{g}^{R,A}(\omega, \epsilon=0)$, with the density of impurities n_i and the strength of the potential u leading to the lifetime $\tau := (v\hbar^2/n_i u^2)$ and the mean free path $\ell := v\tau$. Then, we calculate the retarded and advanced Green's functions through

$$\hat{G}^{R,A} = \hat{G}_{\text{pure}}^{R,A} + \hat{G}_{\text{pure}}^{R,A} \star \hat{\Sigma}^{R,A} \star \hat{G}^{R,A}.$$

Finally, the lesser Green's function is obtained as

$$\hat{G}^< \cong f_F \star \hat{G}^A - \hat{G}^R \star f_F + \hat{G}^R \star [f_F \star \hat{\mathcal{L}}] \star \hat{G}^A$$

with the Fermi distribution function $f_F(\omega)$. Here, we neglect a vertex correction since it gives only a minor correction.²⁵

The self-consistent mean-field gap equation of Δ for a given interaction strength g is given by

$$\frac{1}{g} \Delta = \overline{\langle c_{p,R}^\dagger c_{p,L} \rangle} / 2 \equiv \int \frac{d\omega}{4i\pi} \frac{dp}{2\pi\hbar} \text{tr}[\hat{\sigma}^x \hat{G}^<(\omega, p)], \quad (4)$$

the right-hand side of which is a function of the electric field E and the gap Δ itself. Throughout this paper, we take $g = 5\hbar v$. The solution is obtained by the crossings of the straight line Δ/g and the curve for $\langle c_{p,R}^\dagger c_{p,L} \rangle / 2$ in Fig. 2(a). There exist three regions of the strength of the electric field: (I) $E < E_1$, (II) $E_1 < E < E_2$, and (III) $E > E_2$, where the number of solutions to Eq. (4) is two, three, and one, respectively. Note that the stability of each solution is determined by the condition $\partial(\langle c_{p,R}^\dagger c_{p,L} \rangle / 2) / \partial\Delta < 1/g$. Thus, in region I, the

finite- Δ solution is the only stable one. In Fig. 2(a), we show the case of the equilibrium ($E=0$) with the gap Δ_0 . In region II, there are two stable solutions, i.e., $\Delta=0$ and $\Delta \neq 0$, as shown for the case of $\zeta/\xi = eE\hbar v / 4\Delta_0^2 = 0.8$ in Fig. 2(a), except the intermediate unstable one. This is the typical situation of the first-order phase transition. In region III, the stability of the $\Delta \neq 0$ solution is lost, and the metallic state ($\Delta=0$) becomes the only stable solution, as shown for the case of $\zeta/\xi = 1.2$ in Fig. 2(a). Therefore, we conclude that the spin/charge ordered system shows the first-order-like switching phenomenon.

We argue that these two threshold electric fields are essentially given by $E_1 = \Delta_0 / e v \tau$ and $E_2 = \Delta_0^2 / e \hbar v$. It is easy to understand that E_2 is the Zener breakdown field since at $E > E_2$, the gap does not prevent the metallic current flow and hence the insulating state is unstable. To understand why the lower threshold field E_1 appears, it is useful to consider the instability of the metallic current-carrying state. The steady state with the current is characterized by the shift of the electron distribution function by an amount of $\delta k = eE\tau$, with $\tau = \ell / v$ being the mean free time. With this shift, the energy difference between the right- and left-moving electrons at the shifted Fermi level is $\delta\epsilon = 2v\delta k$. When this energy is larger than the gap $2\Delta_0$ in the equilibrium state, the instability toward the spin-density wave (SDW)/charge-density wave (CDW) disappears. This consideration leads to the estimation $E_1 = \Delta_0 / e v \tau$, which is smaller than the Zener breakdown field $E_2 = \Delta_0^2 / e \hbar v$ by a factor of $\hbar / (\tau\Delta_0) \ll 1$.

Now we study the physical properties associated with the switching phenomenon. Of the most importance is the I - E characteristics. The current I flowing through the sample is obtained from the relation

$$I = \frac{e^2 v^2 E}{2} \int \frac{d\omega}{2\pi} \frac{dp}{2\pi} \text{tr} \left[\hat{\sigma}^z \hat{G}^R \star \left(-\hat{\sigma}^z \frac{\partial f_F}{\partial \omega} \right) \star \hat{G}^A \right]. \quad (5)$$

Figure 2(b) shows the I - E characteristics corresponding to the first-order phase transition of the order parameter obtained in Fig. 2(a). There occurs the jump of the current, the upper branch of which corresponds to the metallic conduction while the lower branch corresponds to that of the Zener tunneling in the insulating state. The two threshold electric fields E_1 and E_2 can be separated by a factor as discussed above, and the change in the current is by a factor of $\sim \exp(4\Delta^2 / e\hbar v E)$.

We also propose the measurement of the local density of states (LDOS) in terms of scanning tunneling spectroscopy (STS) to study the nonequilibrium state. Based on the formula for the tunneling current given by Meir and Wingreen,²⁶ we have calculated the STS LDOS as shown in Fig. 3. There appears a peak at the middle of the gap whose height is proportional to the tunneling current. Namely, the tunneling occurs through the in-gap density of states induced by the electric field. In the metallic state after the switching, of course the gap completely closes.

Now the semiquantitative estimation for the realistic situation is in order. Typically, 2Δ is on the order of 1 eV, while \hbar/τ is ~ 10 meV, which leads to the factor of ~ 100 reduction in the switching threshold from the Zener breakdown

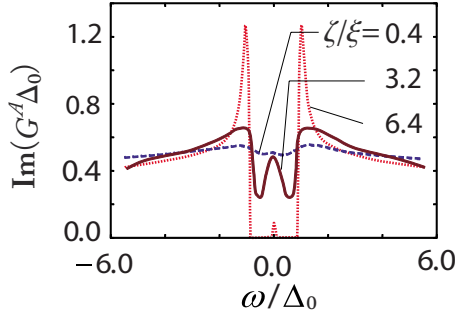


FIG. 3. (Color online) The $\text{Im}(G^A \Delta_0)$ as a function of the normalized energy ω/Δ_0 (Δ_0 : the energy gap in the equilibrium) for $\zeta/\xi=6.4$ (dotted line), 3.2 (solid line), and 0.4 (dashed line) ($\zeta=\hbar v/2\Delta_0$; correlation length, $\xi=2\Delta_0/eE$).

field $\sim 10^6$ V/cm. Therefore, the observed values on the order of 10^4 V/cm (Refs. 9 and 10) is in the reasonable range as expected from the present consideration. The threshold current density j_1 is estimated as $j_1 \sim (\Delta n a)(e/\hbar)$, where n denotes the density of the electron. By using the typical values, we estimate the current density as $j_1 \sim 10^8$ A/cm². This is a very large current density and can be usually realized only in the pulse current experiment since the huge heat generation makes the sample burn out.

However, the breakdown and switching occur often in the filamentary paths of metallic regions.^{5,12} As mentioned above, the emerging in-gap state is associated with the tunneling. In real materials, there are often in-gap states due to the impurities, vacancies, etc., even without the electric field. Suppose there is an impurity level in the gap as shown by the green peak at $R=R_{\text{imp}}$ in Fig. 1. Let t_1 be the tunneling amplitude from the valence band at $R=R_1$ to the impurity level, while t_2 be that from there to the conduction band at $R=R_2$. Note that t_1 and t_2 are exponentially small, i.e., $t_1 \sim \exp[-\pi(R_{\text{imp}}-R_1)/2\zeta]$ and $t_2 \sim \exp[-\pi(R_2-R_{\text{imp}})/2\zeta] \ll 1$, with the product $t_1 t_2$ being the Zener tunneling amplitude without the resonant level. Considering the two barrier problem with the small tunneling amplitudes of t_1 and t_2 , the tunneling probability through the two barriers has the peak height given by $T_{\text{max}} \cong [2t_1 t_2 / (t_1^2 + t_2^2)]^2$ within the narrow energy width $\delta\varepsilon \cong W(t_1^2 + t_2^2)$, which can be translated into the width in the real space $\delta R \cong \delta\varepsilon/(eE)$ in Fig. 1. When the extent of the electron wave packet is larger than δR (which is the case in the limit of small tunneling amplitude), the averaged tunneling probability is on the order of $t_1^2 t_2^2 / (t_1^2 + t_2^2)$. This is much larger than that without the impurity level, i.e., $(t_1 t_2)^2$ corresponding to the tunneling amplitude $t_1 t_2$ for the Zener tunneling. This means that there appear “hot spots” at R_1 and R_2 which are spatially separated by ζ . Therefore the impurities act as the nucleation centers of the nonequilibrium first-order metal-insulator phase transition discussed above. With the random configuration of the impurities, the current can find the path along where these nucleation centers popu-

late densely compared with the other spatial region. This leads to the filamentary paths of the metallic regions as observed experimentally.

Since the width of the filamentary path is given by the correlation length ζ , which characterizes also the spatial variation of the SDW/CDW order parameter, the threshold current I_1 is estimated as $I_1 \sim \pi \zeta^2 j_1 = (\pi n a^2 v / \Delta)(\pi e \hbar) \sim 1 \mu\text{A}$. From this expression, we found that the switching occurs with rather tiny current in correlated insulators. Moreover, from the point of view of the Joule heating, the correlated insulator is more advantageous over semiconductors. The Joule heat corresponding to the breakdown is written as $P = j_1 E_1 = (\Delta a)^2 (1/\hbar v \tau)$. For the correlated insulator, this is estimated as $P_{\text{cor}} \sim 10^{12}$ V A/cm³. This value is rather similar to that in the typical semiconductors. However, as mentioned above, the current is confined within filaments of nanoscale in the correlated systems, while it is rather uniformly distributed in semiconductors. Therefore, the total heat generation P'_{cor} is expected to be much smaller in the correlated insulator as $P'_{\text{cor}} = \varrho \pi \zeta^2 j \sim \varrho \times 10^{-2}$ V A/cm³, where ϱ denotes the density of the filaments. Once some filaments appear, the voltage drop across the sample disappears and no additional filaments are needed.

In Ref. 13, the zero-temperature threshold electric field for Sr₂CuO₃ and SrCuO₂ is estimated as 10^6 – 10^7 V/cm by the extrapolation of the data at finite temperature (~ 100 K) (Ref. 10). In the case of La_{2-x}Sr_xNiO₄,⁹ on the other hand, the temperature dependence of the threshold field can be fitted to $\propto \exp(-T/T_0)$ with a certain parameter T_0 at low temperature showing a saturation value on the order of $\sim 10^4$ V/cm. Therefore, we have at least one example where the threshold field is much smaller than the simple estimation from the Zener tunneling formula. However, the study of the temperature dependence of the threshold field, which requires the treatment of the fluctuation beyond the mean-field theory, is left for future investigations.

To summarize, we have studied the switching phenomenon of the correlated insulator under an applied electric field. Due to the feedback effect of the current on the spin/charge ordering, the switching occurs with much weaker field/smaller current/smaller heat generation as compared with those expected from the simple Zener breakdown picture. This finding will be useful for the future application of this phenomenon to memory and switching devices.

S.O. thanks S. Okamoto for discussion. The work was partly supported by Grants-in-Aid No. 15104006, No. 16076205, No. 17105002, and No. 19048015, under the NAREGI Nanoscience Project from the Ministry of Education, Culture, Sport, Science and Technology (MEXT), Japan and the Global COE Program “The Physical Sciences Frontier.” S.O. was supported by Grant-in-Aid No. 19840053 from the Japan Society of the Promotion of Science.

*sugimoto@appi.t.u-tokyo.ac.jp

- ¹ *Colossal Magnetoresistive Oxides*, Advances in Condensed Matter Science Vol. 2, edited by Y. Tokura (Gordon and Breach, Amsterdam, 2000).
- ² S. M. Sze and K. Ng. Kwok, *Physics of Semiconductor Devices*, 3rd ed. (Wiley, New York, 2007).
- ³ N. F. Mott, *Metal-Insulator Transitions* (Taylor & Francis, London, 1990).
- ⁴ A. Asamitsu, Y. Tomioka, H. Kuwahara, and Y. Tokura, *Nature (London)* **388**, 50 (1997).
- ⁵ N. Takubo and K. Miyano, *Phys. Rev. B* **76**, 184445 (2007).
- ⁶ K. Miyano, T. Tonogai, T. Satoh, H. Oshima, and Y. Tokura, *J. Phys. IV* **9**, Pr10–311 (1999).
- ⁷ K. Miyano, T. Tanaka, Y. Tomioka, and Y. Tokura, *Phys. Rev. Lett.* **78**, 4257 (1997).
- ⁸ R. Kumai, Y. Okimoto, and Y. Tokura, *Science* **284**, 1645 (1999).
- ⁹ S. Yamanouchi, Y. Taguchi, and Y. Tokura, *Phys. Rev. Lett.* **83**, 5555 (1999).
- ¹⁰ Y. Taguchi, T. Matsumoto, and Y. Tokura, *Phys. Rev. B* **62**, 7015 (2000).
- ¹¹ A. Sawa, T. Fujii, K. Kawasaki, and Y. Tokura, *Appl. Phys. Lett.* **85**, 4073 (2004).
- ¹² J. Burgoyne, E. Dagotto, and M. Mayr, *Phys. Rev. B* **67**, 014410 (2003). The authors studied a metal-insulator transition in the equilibrium state. On the other hand, we study the instability of the insulator induced by the strong electric field.
- ¹³ T. Oka and N. Nagaosa, *Phys. Rev. Lett.* **95**, 266403 (2005); T. Oka, R. Arita, and H. Aoki, *ibid.* **91**, 066406 (2003); T. Oka and H. Aoki, *ibid.* **95**, 137601 (2005); arXiv:0803.0422 (unpublished), and references therein. This paper is a draft of a chapter of the book entitled *Quantum and Semi-Classical Percolation and Breakdown*, Lecture Notes in Physics (LNP) (Springer-Verlag, Berlin, to be published.).
- ¹⁴ S. Okamoto and A. J. Millis, *Nature (London)* **428**, 630 (2004), and references therein.
- ¹⁵ S. Okamoto, *Phys. Rev. B* **76**, 035105 (2007).
- ¹⁶ S. Onoda, N. Sugimoto, and N. Nagaosa, *Prog. Theor. Phys.* **116**, 61 (2006).
- ¹⁷ G. Gruner, *Density Waves in Solids*, Advanced Book Program (Perseus, Cambridge, MA, 2000).
- ¹⁸ L. D. Landau, *Phys. Z. Sowjetunion* **2**, 46 (1932).
- ¹⁹ C. Zener, *Proc. R. Soc. London, Ser. A* **A137**, 696 (1932).
- ²⁰ E. C. G. Stueckelberg, *Helv. Phys. Acta* **5**, 369 (1932).
- ²¹ Y. Gefen, E. Ben-Jacob, and A. O. Caldeira, *Phys. Rev. B* **36**, 2770 (1987).
- ²² P. Ao and J. Rammer, *Phys. Rev. B* **43**, 5397 (1991).
- ²³ J. M. Ziman, *Principles of the Theory of Solids* (Cambridge University Press, Cambridge, England, 1972), p. 190.
- ²⁴ N. Sugimoto, S. Onoda, and N. Nagaosa, *Prog. Theor. Phys.* **117**, 415 (2007).
- ²⁵ G. Rikayzen, *Green's Functions and Condensed Matter* (Academic, London, 1980), pp. 109–119.
- ²⁶ Y. Meir and N. S. Wingreen, *Phys. Rev. Lett.* **68**, 2512 (1992).